Received: 12 March 2021 | Revised: 1 June 2021 | Accepted: 2 June 2021

DOI: 10.1111/mmi.14765

RESEARCH ARTICLE

WILEY

DNA damage checkpoint activation affects peptidoglycan synthesis and late divisome components in *Bacillus subtilis*

Emily A. Masser | Peter E. Burby | Wayne D. Hawkins | Brooke R. Gustafson | Justin S. Lenhart | Lyle A. Simmons

Department of Molecular, Cellular, and Developmental Biology, University of Michigan, Ann Arbor, MI, USA

Correspondence
Lyle A. Simmons, Department of Molecular, Cellular, and Developmental Biology, University of Michigan, Ann Arbor, MI 48109-1055, USA.
Email: lasimm@umich.edu

Funding information
National Science Foundation, Grant/Award Number: DGE1256260; National Institute of General Medical Sciences, Grant/Award Number: GM131772

Abstract

During normal DNA replication, all cells encounter damage to their genetic material. As a result, organisms have developed response pathways that provide time for the cell to complete DNA repair before cell division occurs. In *Bacillus subtilis*, it is well established that the SOS-induced cell division inhibitor YneA blocks cell division after genotoxic stress; however, it remains unclear how YneA enforces the checkpoint. Here, we identify mutations that disrupt YneA activity and mutations that are refractory to the YneA-induced checkpoint. We find that YneA C-terminal truncation mutants and point mutants in or near the LysM peptidoglycan binding domain render YneA incapable of checkpoint enforcement. In addition, we develop a genetic method which isolated mutations in the *ftsW* gene that completely bypassed checkpoint enforcement while also finding that YneA interacts with late divisome components FtsL, Pbp2b, and Pbp1. Characterization of an FtsW variant resulted in considerably shorter cells during the DNA damage response indicative of hyperactive initiation of cell division and bypass of the YneA-enforced DNA damage checkpoint. With our results, we present a model where YneA inhibits septal cell wall synthesis by binding peptidoglycan and interfering with interaction between late arriving divisome components causing DNA damage checkpoint activation.

KEYWORDS
cell division, DNA damage checkpoint, FtsW, YneA

1 | INTRODUCTION

When cells undergo DNA replication, they encounter a variety of spontaneous and environmental factors that damage their DNA (Friedberg et al., 2006). As a result, organisms from bacteria to humans have developed response pathways that halt cell cycle progression allowing time for accurate DNA repair to take place before cell division occurs (Bridges, 1995; Ciccia & Elledge, 2010; Simmons et al., 2007, 2008; Sutton et al., 2000). It is well established that eukaryotic cells induce expression of cell cycle checkpoints to delay cell cycle progression in response to DNA damage (for review, see Ciccia & Elledge, 2010). However, the process by which different bacterial species respond to genotoxic stress and pause cell cycle progression remains incompletely understood.

In bacteria, cells respond to DNA damage by activating the SOS response (Simmons et al., 2008; Sutton et al., 2000; Walker et al., 2000). This response pathway results in the upregulation of a variety of genes that relieve cellular stress and promote cell survival (Simmons et al., 2008; Sutton et al., 2000; Walker et al., 2000). Following DNA damage in *Escherichia coli*, RecA binds to single-stranded DNA, which promotes autocleavage of the LexA transcriptional repressor, and subsequent activation of the SOS regulon (Lenhart et al., 2012; Little, 1983; Sutton et al., 2000). The SOS regulated cytoplasmic cell division inhibitor SulA delays cell cycle

progression by directly interacting with and preventing the polymerization of FtsZ (Cole, 1983; Mizusawa et al., 1983; Mukherjee et al., 1998). After the DNA has been repaired, SulA is degraded by Lon protease and cell proliferation resumes (Mizusawa & Gottesman, 1983; Mukherjee et al., 1998). While this process is well understood in *E. coli*, the mechanism used by many other bacteria remains partially understood particularly the mechanisms used to prevent cell division or release checkpoint enforcement.

Recently, it has become clear that the SulA-type DNA damage checkpoint enforcement mechanism is of limited conservation among bacteria (for review, see Bojer et al., 2020; Burby & Simmons, 2020). In other bacterial species the DNA damage-induced cell division inhibitor is a small membrane binding protein (Bojer et al., 2020; Burby & Simmons, 2020; Modell et al., 2011). The best understood example of this conserved bacterial DNA damage checkpoint has been described for *Caulobacter crescentus*. *Caulobacter* contains SidA and DidA two DNA damage-inducible cell division inhibitors (Modell et al., 2011, 2014). Both SidA and DidA are small membrane binding proteins that halt cell division following exposure to DNA damage (Modell et al., 2011, 2014). SidA and DidA delay cell proliferation by preventing FtsW, FtsI, and FtsN from forming a subcomplex that is essential for peptidoglycan synthesis at mid-cell (Modell et al., 2011, 2014).

In *Bacillus subtilis*, the SOS-dependent cell division inhibitor YneA blocks cell proliferation after exposure to genotoxic stress (Kawai et al., 2003). In the absence of damage, YneA accumulation is tightly controlled by the checkpoint recovery proteases, DdcP and CtpA, and the DNA damage checkpoint antagonist, DdcA (Burby et al., 2018, 2019). When cells are exposed to agents that halt DNA replication, YneA must reach a critical threshold to overcome these three negative regulators to activate the DNA damage checkpoint (Burby et al., 2018, 2019). After the damage is repaired, YneA is then degraded by membrane-bound proteases CtpA and DdcP allowing for cell division to resume (Burby et al., 2018). The process of controlling YneA expression and degradation is well understood; however, the mechanism underlying how YneA inhibits cell division or how cells can circumvent YneA function remains unknown.

To understand how YneA delays cell division, we used several genetic approaches to identify mutations that disrupt YneA function and extragenic mutations that bypass YneA activity. We identify mutations in *yneA* that prevent function including point mutations in the LysM peptidoglycan binding domain. We also isolated extragenic mutations in the *ftsW* gene encoding a peptidoglycan polymerase that are refractory to YneA activity. Characterization of one FtsW variant shows cell division initiates hyperactively under conditions of DNA damage bypassing the YneA-enforced checkpoint. Further, we show that ectopic or DNA damage induced expression of YneA strongly sensitizes cells to the cell wall antibiotic cephalexin, and we show that YneA interacts with late divisome components FtsL, Pbp2b, and Pbp1. With these results, we present a new model for YneA function where it induces checkpoint enforcement by binding peptidoglycan through its LysM domain while also interacting with and inhibiting late arriving cell division and septal cell wall synthesis proteins FtsL, Pbp2b, and Pbp1.

2 | RESULTS

2.1 | yneA C-terminal truncations impair checkpoint activation

Previous work identified a point mutation within the C-terminal tail (*D95A*) of *yneA* that caused an increase in YneA activity (Mo & Burkholder, 2010). Further, it was shown that C-terminal truncations of *Staphylococcus aureus* SosA resulted in increased growth interference (Bojer et al., 2019). A distinct difference between SosA and YneA is that YneA contains a LysM domain and SosA does not (Bojer et al., 2019). Therefore, we asked if the 15 amino acid C-terminal tail present after the LysM domain is required for YneA to block cell division in *B. subtilis*. We generated C-terminal truncations of YneA that lack the last five (*yneA*Δ*5*), 10 (*yneA*Δ*10*), or 15 (*yneA*Δ*15*) amino acid residues with the Δ*15* truncation located near the predicted LysM domain boundary (Figure 1a; Mo & Burkholder, 2010). We placed these truncations under the control of a highly induced isopropyl β-D-1-thiogalactopyranoside (IPTG) regulated promoter (P_{hy}) and integrated each allele at the ectopic *amyE* locus. We used an IPTG regulated promoter to uncouple *yneA* expression from the SOS response so that we could induce *yneA* without adding DNA damage and inducing expression of the other ~64 genes in the SOS regulon (Au et al., 2005). We ectopically expressed wild type (WT) *yneA* and each *yneA* truncation mutant in a strain that lacks endogenous *yneA* (Δ*yneA::loxP*; Figure 1b). We show that cells are highly sensitive to *yneA* overexpression in the absence of endogenous *yneA* (Figure 1b). However, when we induced expression of *yneA*Δ*5* or *yneA*Δ*10*, cell proliferation was partially impaired, showing more growth than WT *yneA*, but less growth compared to cells grown in the absence of induced *yneA* expression (Figure 1b). Interestingly, in cells expressing *yneA*Δ*15* growth was the same as that observed in cells lacking the IPTG induced *yneA* gene or cells with P_{hy}-*yneA* grown in the absence of IPTG (Figure 1b). These results show that the C-terminal 15 amino acids are required for checkpoint enforcement.

Previous work showed that cells are more sensitive to *yneA* overexpression when they lack a single checkpoint recovery protease (Burby et al., 2018). As a result, we asked if overexpression of the *yneA* C-terminal truncation mutants caused sensitivity when expressed in the Δ*ddcP*-single protease mutant background. We show that cells are more sensitive to *yneA* overexpression in the Δ*ddcP* protease mutant background compared to expression in the *yneA* null strain (Figure 1b,c). Two C-terminal truncations also showed a sensitive overexpression phenotype in the protease mutant background (Figure 1b,c). Overexpression of the *yneA*Δ*5* or *yneA*Δ*10* truncation caused moderate growth interference, while *yneA*Δ*15* truncation mutant was completely benign (Figure 1c). Importantly, these results show that the C-terminal amino acids of YneA are important for activity and that these alleles do not confer a more toxic expression phenotype as observed for the *S. aureus* SosA C-terminal truncation mutants lacking the last 10 or 20 amino acid residues (Bojer et al., 2019). Further, our results show that loss of the C-terminal 15 amino acids of YneA completely blocks checkpoint

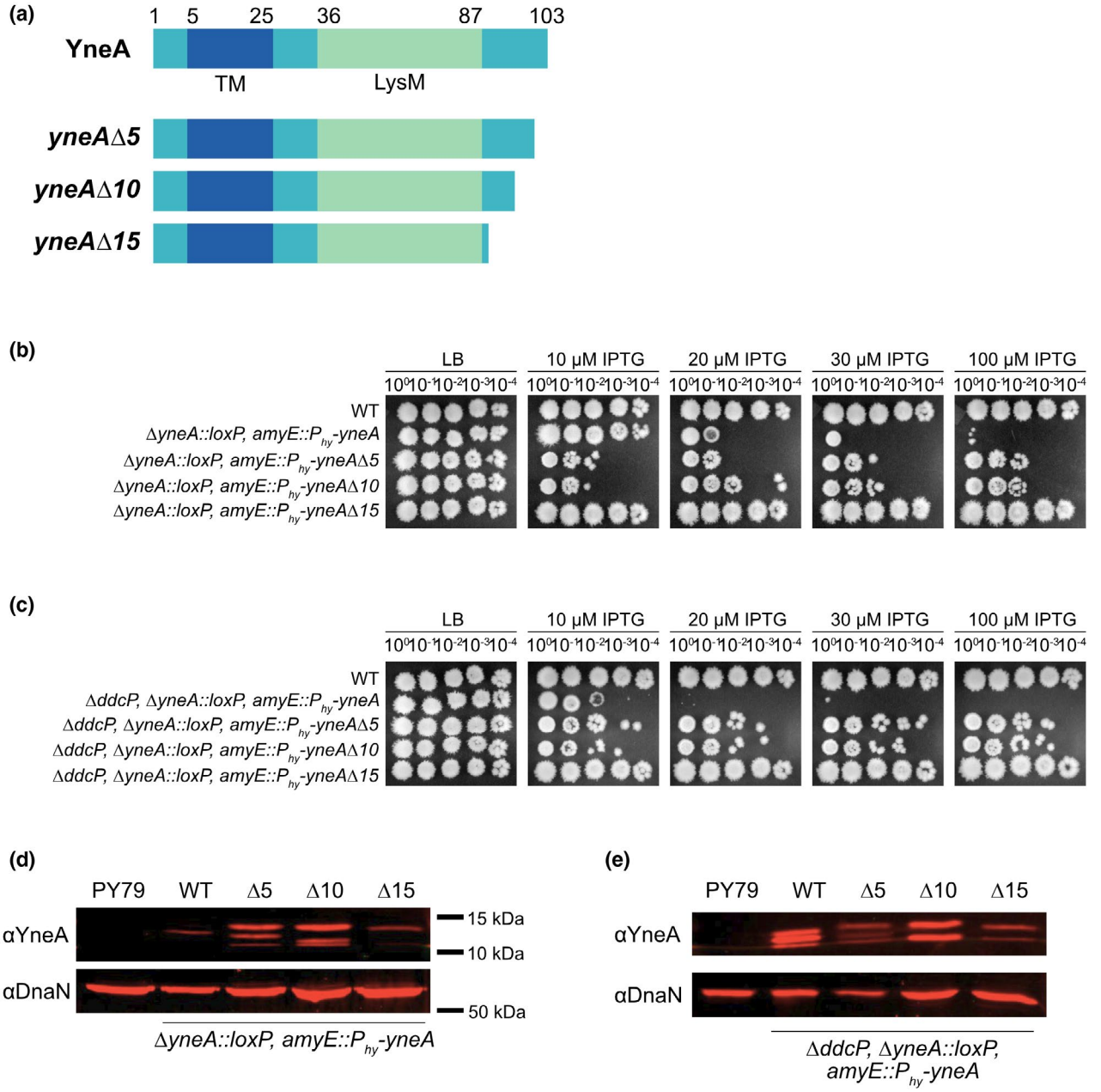

FIGURE 1 *yneA* C-terminal truncations impair checkpoint activation. (a) Schematic of the full-length YneA protein and the C-terminal truncation mutants lacking the last five (*yneAΔ5*), 10 (*yneAΔ10*), and 15 (*yneAΔ15*) amino acid residues. YneA is predicted to have a transmembrane domain (TM) and a LysM domain (LysM). (b) Spot titer assay using *B. subtilis* strains WT (PY79), Δ*yneA::loxP amyE::*P_{hy}*-yneA* (EAM46), Δ*yneA::loxP amyE::*P_{hy}*-yneAΔ5* (EAM53), Δ*yneA::loxP amyE::*P_{hy}*-yneAΔ10* (EAM54), and Δ*yneA::loxP amyE::*P_{hy}*-yneAΔ15* (EAM55) spotted on the indicated media. (c) Spot titer assay using *B. subtilis* strains WT (PY79), Δ*ddcP* Δ*yneA::loxP amyE::*P_{hy}*-yneA* (EAM48), Δ*ddcP* Δ*yneA::loxP amyE::*P_{hy}*-yneAΔ5* (EAM83), Δ*ddcP* Δ*yneA::loxP amyE::*P_{hy}*-yneAΔ10* (EAM84), and Δ*ddcP* Δ*yneA::loxP amyE::*P_{hy}*-yneAΔ15* (EAM85) spotted on the indicated media. (d) Western blot using antisera against YneA (upper panel) or DnaN (lower panel) using *B. subtilis* strains WT (PY79), Δ*yneA::loxP amyE::*P_{hy}*-yneA* (EAM46), Δ*yneA::loxP amyE::*P_{hy}*-yneAΔ5* (EAM53), Δ*yneA::loxP amyE::*P_{hy}*-yneAΔ10* (EAM54), and Δ*yneA::loxP amyE::*P_{hy}*-yneAΔ15* (EAM55) after growing in the presence of IPTG until an $OD_{600} = 1$. (e) Western blot using antisera against YneA (upper panel) or DnaN (lower panel) using *B. subtilis* strains WT (PY79), Δ*ddcP* Δ*yneA::loxP amyE::*P_{hy}*-yneA* (EAM48), Δ*ddcP* Δ*yneA::loxP amyE::*P_{hy}*-yneAΔ5* (EAM83), Δ*ddcP* Δ*yneA::loxP amyE::*P_{hy}*-yneAΔ10* (EAM84), and Δ*ddcP* Δ*yneA::loxP amyE::*P_{hy}*-yneAΔ15* (EAM85) after growing in the presence of IPTG until an $OD_{600} = 1$

enforcement indicating that complete YneA clearance is not required for cell division to resume.

Given that the C-terminal truncations attenuated the growth interference of *yneA* expression in both the Δ*yneA::loxP* and Δ*yneA::loxP*, Δ*ddcP* backgrounds, we asked if YneA protein levels changed when the truncation mutants were overexpressed. When YneA is examined by western blot, multiple bands are observed because the protein is cleaved by proteases generating different

sizes (Burby et al., 2018). In the Δ*yneA::loxP* background, we observed an increase in YneA expression when *yneAΔ5* and *yneAΔ10* truncation mutants were induced relative to WT. This result indicates that although the YneAΔ5 and YneAΔ10 variants accumulate to levels higher than WT, they are less toxic than WT YneA when IPTG concentrations are increased. The stabilization of YneAΔ5 and YneAΔ10 further suggests that both variants are less susceptible to proteolytic digestion by DdcP and CtpA although the deletion of these C-terminal residues impairs YneA checkpoint enforcement. To gain more insight into the susceptibility of the YneA C-terminal truncations to proteolytic cleavage, we completed western blots of YneA, YneAΔ5, YneAΔ10, and YneAΔ15 in lysates prepared from cells lacking DdcP (Δ*ddcP*; Figure 1e). We show that induction of YneAΔ15 caused a reduction in YneA expression in the Δ*ddcP* background as well. We find a lower abundance of YneAΔ15 as compared with WT or YneAΔ10 (Figure 1e). With this data, we suggest that YneA is less stable without the last 15 amino acids, and this truncation is completely ineffective at inducing the DNA damage checkpoint. In conclusion, we show that once YneA has lost its C-terminal 15 amino acids, it is inactivated demonstrating that protease cleavage of the C-terminal residues is sufficient to inactivate YneA and allow for cell division to resume without requiring complete clearance of the protein. This observation provides a mechanism for efficient inactivation of the DNA damage checkpoint after YneA expression is repressed and the C-terminus is cleaved by DdcP or CtpA (Burby et al., 2018).

2.2 | Isolation of mutations in YneA that prevent checkpoint activation

Given our results above showing the importance of the C-terminal residues to YneA activity, we chose to identify single residues critical for checkpoint enforcement using a genetic selection. We show in Figure 1 that *B. subtilis* cells are strongly growth impaired when ectopic expression of *yneA* occurs from an IPTG regulated promoter. This provides an assay to select for mutations in *yneA* that fail to enforce the DNA damage checkpoint with the potential to identify the most important characteristics of YneA that are required for checkpoint activation (Figure 2a). Therefore, we selected for colonies that were able to grow on LB plates containing IPTG to induce expression of WT *yneA* (Figure 2a). We identified three mutations in the *yneA* gene located in two functional domains (Figure 2b; Mo & Burkholder, 2010). One mutation is located in the transmembrane domain and two mutations are located in the LysM peptidoglycan binding domain. Mutations in the transmembrane domain have been extensively studied in prior work (Mo & Burkholder, 2010), while mutations in the LysM domain have not been studied and only truncation of the entire LysM domain has been reported to inactivate YneA (Mo & Burkholder, 2010). The important point from this selection is that our unbiased approach has identified 3-point mutations within two regions, which appear to render YneA incapable of checkpoint enforcement.

To functionally assess the novel *yneA* alleles, we cloned each and placed the alleles in *B. subtilis* at an ectopic locus in a clean genetic background and performed spot titer assays to determine if these mutations render YneA incapable of blocking cell division (Figure 2c,d). We ectopically induced expression of each allele with increasing concentrations of IPTG in the absence of native *yneA* (Δ*yneA::loxP*). We found that each *yneA* allele was impaired or completely broken for checkpoint enforcement even in conjunction with deletion of the checkpoint recovery protease *ddcP* (Δ*yneA::loxP*, Δ*ddcP*; Figure 2c,d). These results establish that induced expression of all three mutants renders *yneA* incapable of causing a block to cell division (Figure 2c,d).

We directly assessed YneA protein levels using western blotting, to determine if the integrity of the protein variants was compromised (Figure 2e,f). We observed higher expression of WT in the absence of endogenous *ddcP*, as previously established (Burby et al., 2018). We detected a single band when *yneA-G10D* was induced in the *yneA* null background and a complete loss of expression in the absence of endogenous *ddcP* (Figure 2f). Although the reason for poor accumulation of YneAG10D is unclear, it suggests that YneAG10D is either intrinsically unstable or hypersensitive to proteolysis by other proteases in the absence of *ddcP*. We observe an increase in expression of LysM domain YneA variants V68A and G82S relative to WT.

We asked if YneA LysM domain mutants *V68A* and *G82S* are dominant or recessive to SOS induced *yneA*. We found that expression of *yneA V68A* and *G82S* is recessive to SOS induced *yneA* on increasing concentrations of DNA damage (Figure S1). In addition, we created a LysM domain swap where we replaced the YneA LysM domain with the LysM from the *B. subtilis* sporulation protein SafA (Pereira et al., 2019) followed by the YneA C-terminal tail. We found that expression of the *yneA-safA-lysM* chimera failed to interfere with growth demonstrating that the YneA LysM domain is specific for checkpoint enforcement (Figure S2). These results establish the importance of the LysM domain for YneA activity.

2.3 | Cells are more sensitive to yneA induction in the absence of the negative regulators ddcP, ctpA, and ddcA

Previous work established that the checkpoint recovery proteases, DdcP and CtpA, as well as the DNA damage checkpoint antagonist, DdcA, ensure YneA activity is suppressed in the absence of DNA damage (Burby et al., 2018, 2019). Moreover, YneA expression must reach a certain threshold to overcome these negative regulators to activate the checkpoint and inhibit cell division (Burby et al., 2018, 2019). This work also showed that cell proliferation was inhibited when *yneA* was expressed ectopically using xylose induction in the absence of *ddcA*, *ddcP*, and *ctpA* and in the presence of native *yneA* (Burby et al., 2019). We built from these prior studies to clearly establish a system where we could drive *yneA* expression and cause toxicity using either xylose or an IPTG induced promoter (Figure 1b,c). We ectopically expressed *yneA* using an IPTG regulated promoter in cells lacking *ddcA*, *ddcP*,

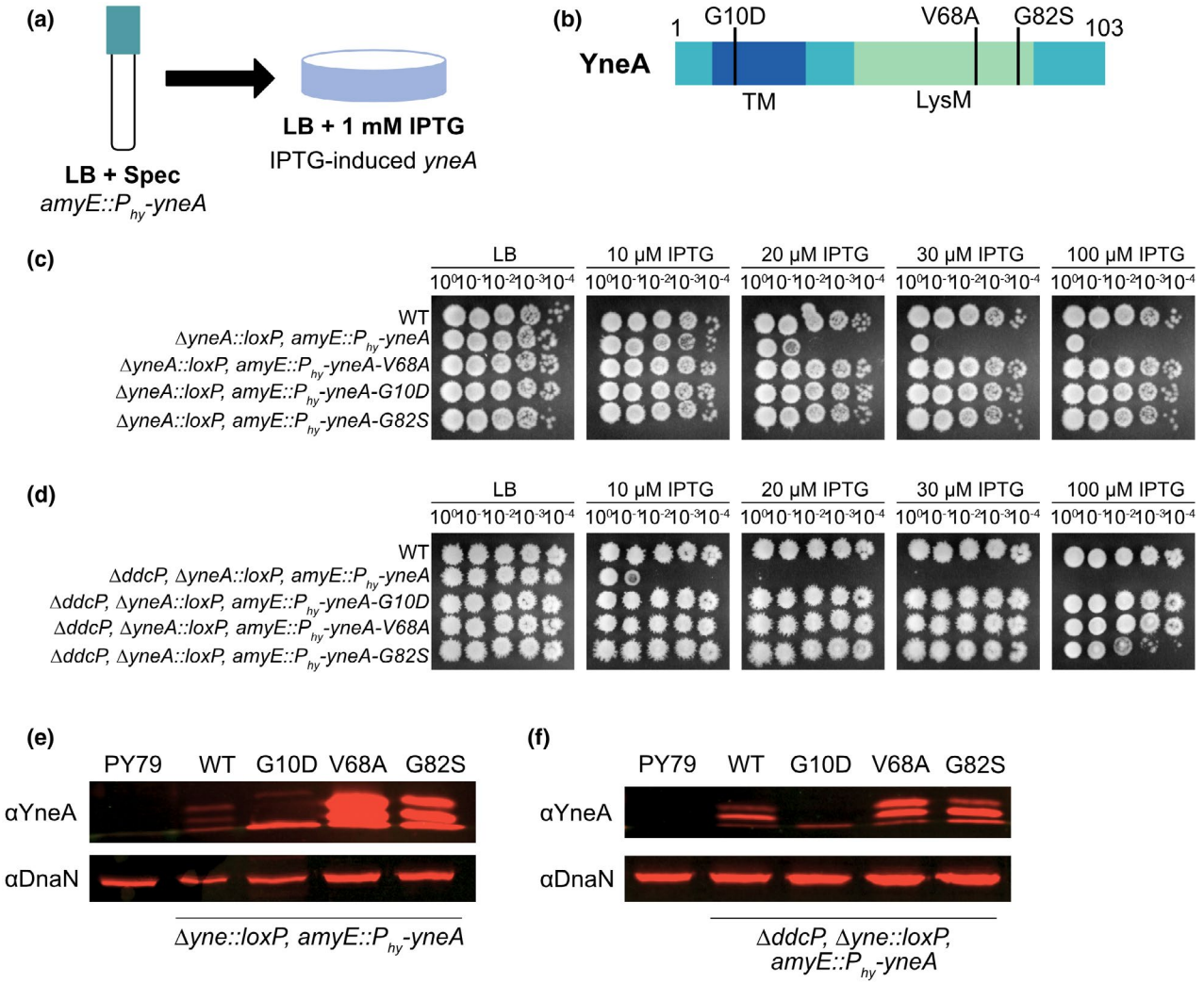

FIGURE 2 Isolation of mutations in *yneA* that prevent checkpoint activation. (a) Experimental design for the primary selection. Cultures were plated on LB agar containing 1 mM IPTG to induce expression of *amyE::P*$_{hy}$*-yneA*. (b) Schematic of the YneA protein and the location of the suppressor mutations identified in the screen. Transmembrane domain (TM) and a LysM domain (LysM). (c) Spot titer assay using *B. subtilis* strains WT (PY79), Δ*yneA::loxP amyE::P*$_{hy}$*-yneA* (EAM46), Δ*yneA::loxP amyE::P*$_{hy}$*-yneA-V68A* (EAM49), Δ*yneA::loxP amyE::P*$_{hy}$*-yneA-G10D* (EAM50), and Δ*yneA::loxP amyE::P*$_{hy}$*-yneA-G82S* (EAM52) spotted on the indicated media. (d) Spot titer assay using *B. subtilis* strains WT (PY79), Δ*ddcP* Δ*yneA::loxP amyE::P*$_{hy}$*-yneA* (EAM48), Δ*ddcP* Δ*yneA::loxP amyE::P*$_{hy}$*-yneA-G10D* (EAM63), Δ*ddcP* Δ*yneA::loxP amyE::P*$_{hy}$*-yneA-V68A* (EAM78), and Δ*ddcP* Δ*yneA::loxP amyE::P*$_{hy}$*-yneA-G82S* (EAM79) spotted on the indicated media. (e) Western blot using antisera against YneA (upper panel) or DnaN (lower panel) using *B. subtilis* strains WT (PY79), Δ*yneA::loxP amyE::P*$_{hy}$*-yneA* (EAM46), Δ*yneA::loxP amyE::P*$_{hy}$*-yneA-V68A* (EAM49), Δ*yneA::loxP amyE::P*$_{hy}$*-yneA-G10D* (EAM50), and Δ*yneA::loxP amyE::P*$_{hy}$*-yneA-G82S* (EAM52) after growing in the presence of IPTG until an $OD_{600} = 1$. (f) Western blot using antisera against YneA (upper panel) or DnaN (lower panel) using *B. subtilis* strains WT (PY79), Δ*ddcP* Δ*yneA::loxP amyE::P*$_{hy}$*-yneA* (EAM48), Δ*ddcP* Δ*yneA::loxP amyE::P*$_{hy}$*-yneA-G10D* (EAM63), Δ*ddcP* Δ*yneA::loxP amyE::P*$_{hy}$*-yneA-V68A* (EAM78), and Δ*ddcP* Δ*yneA::loxP amyE::P*$_{hy}$*-yneA-G82S* (EAM79) after growing in the presence of IPTG until an $OD_{600} = 1$

ctpA, and native *yneA* genes (Figure 3a). As a control we show that growth inhibition does not occur in the absence of *ddcP*, *ctpA*, *ddcA*, and native *yneA*, supporting prior results that growth inhibition is dependent on induced *yneA* expression (Figure 3a; Burby et al., 2019). Therefore, the cell proliferation defect observed with Δ*ddcP*, Δ*ctpA*, Δ*ddcA*, and Δ*yneA::loxP* is caused by induced expression of IPTG regulated *yneA* (Figure 3a; Burby et al., 2018, 2019).

We further investigated the effect of *yneA* expression on cell proliferation by treating cells with increasing concentrations of the DNA damaging agent mitomycin C (MMC) (Iyer & Szybalski, 1963; Noll et al., 2006) to induce native *yneA* in the presence or absence of the IPTG regulated *yneA* allele (Burby et al., 2019; Figure 3b). It was previously shown that YneA inhibits cell division in *B. subtilis* following DNA damage (Burby et al., 2018, 2019; Kawai et al., 2003). As a result, we expect a cell proliferation defect following MMC treatment because endogenous *yneA* should be activated. When we treat cells with increasing concentrations of MMC, we find that cells are sensitive to MMC and this phenotype is more severe in the absence of the *ddcP*, *ctpA*, and *ddcA* negative regulators of YneA (Figure 3b) as described (Burby et al., 2019). If this phenotype is due to induction of

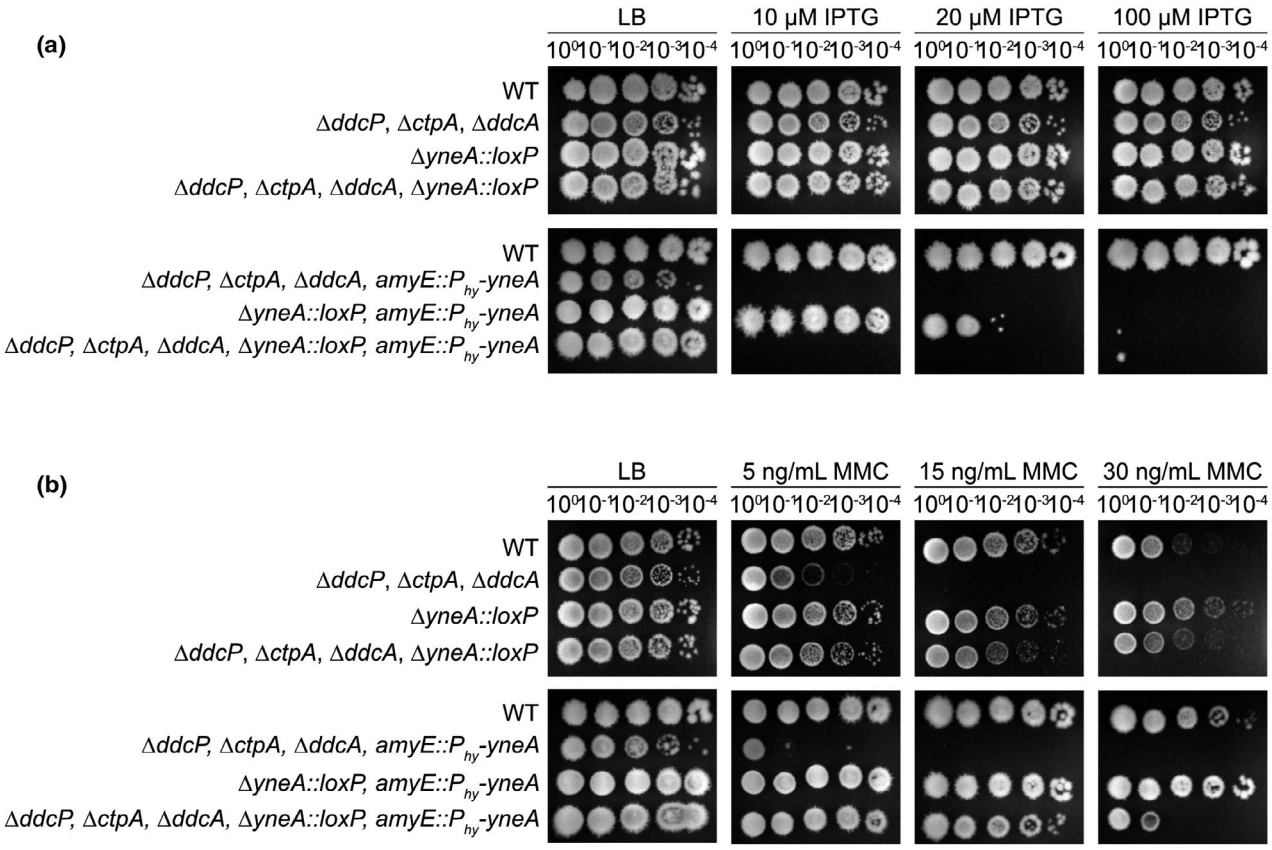

FIGURE 3 Cells are more sensitive to *yneA* induction in the absence of the negative regulators *ddcP*, *ctpA*, and *ddcA*. (a) Spot titer assay using *B. subtilis* strains WT (PY79), Δ*ddcP* Δ*ctpA* Δ*ddcA* (PEB639), Δ*yneA::loxP* (PEB439), Δ*ddcP* Δ*ctpA* Δ*ddcA* Δ*yneA::loxP* (PEB643), Δ*ddcP* Δ*ctpA* Δ*ddcA amyE::P$_{hy}$-yneA* (PEB844), Δ*yneA::loxP amyE::P$_{hy}$-yneA* (EAM46), and Δ*ddcP* Δ*ctpA* Δ*ddcA* Δ*yneA::loxP amyE::P$_{hy}$-yneA* (EAM56) spotted on the indicated media. (b) Spot titer assay using *B. subtilis* strains WT (PY79), Δ*ddcP* Δ*ctpA* Δ*ddcA* (PEB639), Δ*yneA::loxP* (PEB439), Δ*ddcP* Δ*ctpA* Δ*ddcA* Δ*yneA::loxP* (PEB643), Δ*ddcP* Δ*ctpA* Δ*ddcA amyE::P$_{hy}$-yneA* (PEB844), Δ*yneA::loxP amyE::P$_{hy}$-yneA* (EAM46), and Δ*ddcP* Δ*ctpA* Δ*ddcA* Δ*yneA::loxP amyE::P$_{hy}$-yneA* (EAM56) spotted on the indicated media

endogenous *yneA*, then we would expect that loss of the native *yneA* gene should rescue the phenotype. Indeed, we show that cells are able to continue proliferating when treated with MMC in the absence of endogenous *yneA* and in the presence of IPTG regulated *yneA* (uninduced; Figure 3b). As a result, the inability to continue proliferating after MMC treatment is the result of SOS regulated expression of the native *yneA* gene supporting prior observations (Burby et al., 2018, 2019).

These results and those of Burby et al establish that we can inhibit cell proliferation by inducing expression of *yneA* from two different locations in the genome (Burby et al., 2019). Our ability to induce ectopic *yneA* or native *yneA* in the absence of the *yneA* negative regulators establishes a strong selective pressure to isolate mutations outside of the *yneA* gene that are refractory to checkpoint enforcement (see below).

2.4 | ftsW-L148P suppresses YneA activity in the presence of DNA damage

In order to better understand how YneA inhibits cell division, we sought to identify additional factors that are involved in this process. The intent is to isolate extragenic mutations that are refractory to checkpoint enforcement. To achieve this end, we devised a method that takes advantage of *yneA* at two different chromosomal locations under different transcriptional regulatory control as described in Figure 3 and in Burby et al. (2019). We first employed a strain with *yneA* at its native locus under SOS control and *yneA* integrated at the *amyE* locus with expression under xylose control for tight repression to decrease the likelihood of leak expression causing growth interference. Therefore, this method favors mutations outside of the *yneA* gene that will overcome YneA function because to inactivate the *yneA* gene directly would require mutations in two separate copies of *yneA* located at distant chromosomal locations.

Our method identified 25 independent missense mutations that occurred in the *ftsW* gene. A striking feature of this result is that of the 25 mutations identified in the *ftsW* gene only three amino acids were affected and 19 out of 25 changes altered one amino acid residue (Figure 4b). A few other spurious mutations were identified; these mutations only occurred once and are reported in Table S1. We interpret this result to mean that there are a select few mutations outside of *yneA* that can overcome checkpoint enforcement contributing to the reported difficulties in isolating such mutants

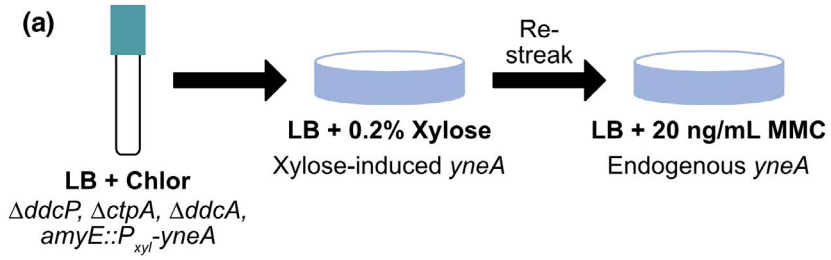

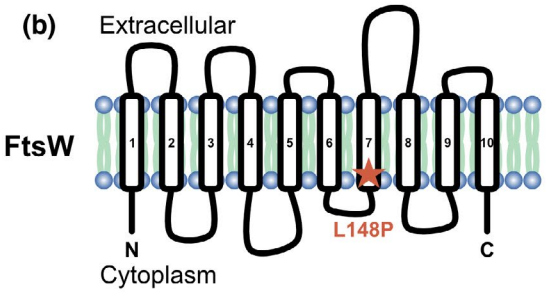

Gene	Mutation	Count
ftsW	L148P (CTG→CCG)	4
	P158L (CCT→CTT)	9
	P158S (CCT→TCT)	11
	A99V (GCC→CTC)	1
	TCACAAGCC insertion at nt 439	1
	TGA insertion at nt 440	2
	CTTGTG insertion at nt 403	1

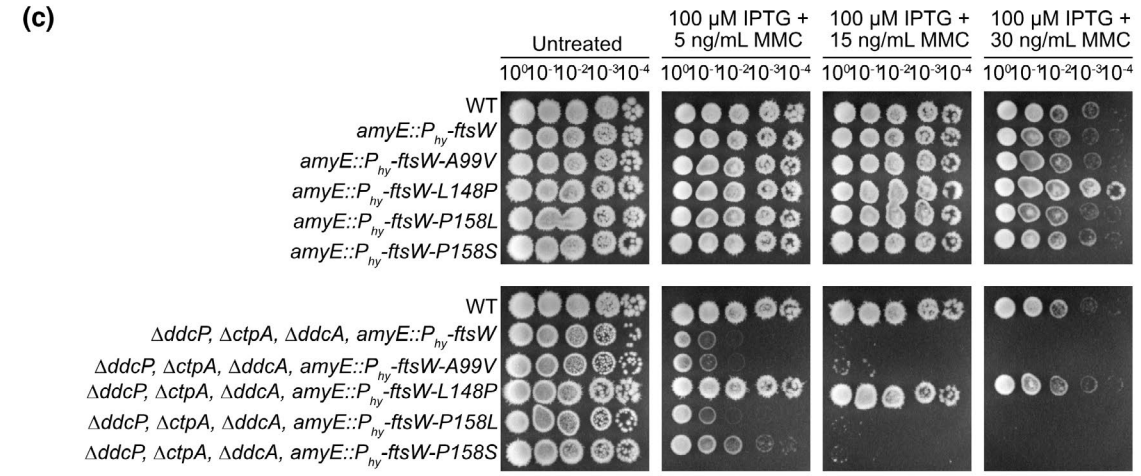

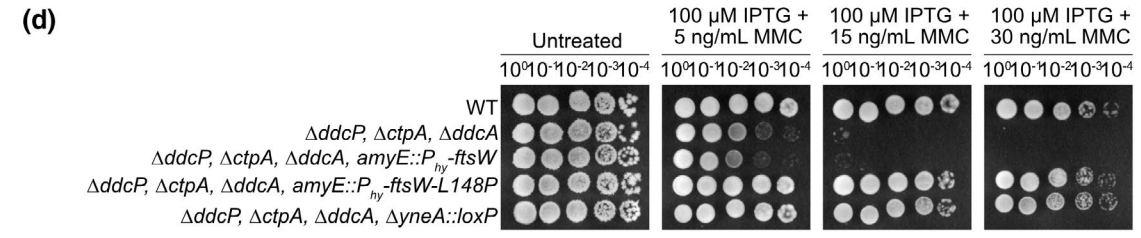

FIGURE 4 *ftsW-L148P* suppresses YneA activity in the presence of DNA damage. (a) Experimental design for the selection followed by secondary screen. Cultures were plated on LB agar containing 0.2% xylose to induce expression of *amyE*::P_{xyl}-*yneA*. Colonies were re-streaked on LB agar containing 20 ng/ml of MMC to induce expression of endogenous *yneA*. (b) Schematic of the FtsW protein and the location of the suppressor mutation identified in the screen. FtsW is a membrane-spanning protein that is predicted to have ten transmembrane segments. Table of the *ftsW* point mutations and insertions identified in the screen. (c) Spot titer assay using *B. subtilis* strains WT (PY79), *amyE*::P_{hy}-*ftsW* (EAM72), *amyE*::P_{hy}-*ftsW-A99V* (EAM68), *amyE*::P_{hy}-*ftsW-L148P* (EAM69), *amyE*::P_{hy}-*ftsW-P158L* (EAM70), *amyE*::P_{hy}-*ftsW-P158S* (EAM71), Δ*ddcP* Δ*ctpA* Δ*ddcA amyE*::P_{hy}-*ftsW* (EAM73), Δ*ddcP* Δ*ctpA* Δ*ddcA amyE*::P_{hy}-*ftsW-A99V* (EAM64), Δ*ddcP* Δ*ctpA* Δ*ddcA amyE*::P_{hy}-*ftsW-L148P* (EAM65), Δ*ddcP* Δ*ctpA* Δ*ddcA amyE*::P_{hy}-*ftsW-P158L* (EAM66), and Δ*ddcP* Δ*ctpA* Δ*ddcA amyE*::P_{hy}-*ftsW-P158S* (EAM67) spotted on the indicated media. (d) Spot titer assay using *B. subtilis* strains WT (PY79), Δ*ddcP* Δ*ctpA* Δ*ddcA* (PEB639), Δ*ddcP* Δ*ctpA* Δ*ddcA amyE*::P_{hy}-*ftsW* (EAM73), Δ*ddcP* Δ*ctpA* Δ*ddcA amyE*::P_{hy}-*ftsW-L148P* (EAM65), and Δ*ddcP* Δ*ctpA* Δ*ddcA* Δ*yneA*::*loxP* (PEB643) spotted on the indicated media

(Mo & Burkholder, 2010). As a follow-up test, we introduced the *ftsW-A99V*, *ftsW-L148P*, *ftsW-P158L*, and *ftsW-P158S* under the control of an IPTG-inducible promoter at an ectopic locus to allow for increased expression in WT and Δ*ddcP*, Δ*ctpA*, and Δ*ddcA* triple mutant backgrounds with native *ftsW* intact. This was done to determine if any of the *ftsW* mutants we isolated are dominant negative to WT *ftsW* as a stringent genetic test for integrity of the variant protein in vivo.

If the FtsW variant bypasses YneA activity and is dominant to WT FtsW, this would provide the best candidate for further characterization. To this end, we asked if each *ftsW* allele was able to suppress the *yneA*-dependent DNA damage checkpoint in the presence of MMC and WT *ftsW*. We found that IPTG-induced *ftsW-L148P* was refractory to YneA in an otherwise WT background or in cells lacking all three YneA negative regulators (Δ*ddcP*, Δ*ctpA*, and Δ*ddcA*; Figure 4c). The triple mutant strain alone is highly sensitive to MMC treatment; however, induction of *ftsW-L148P*, but not *ftsW*, in this background rescues growth (Figure 4d). If this mutation is bypassing YneA activity, then we would expect that the strain expressing *ftsW-L148P* to phenocopy the strain without endogenous *yneA*. Indeed, challenged with MMC, in the absence of endogenous *yneA*, cells are able to continue growth (Figure 4d). We find that IPTG-induced *ftsW-L148P* rescues the sensitivity to MMC and the cell proliferation defect observed in the triple mutant alone. These results establish *ftsW-L148P* as either encoding a form of FtsW that induces hyperactive cell division to bypass YneA inhibition or an FtsW variant that is refractory to negative regulation by impairing direct interaction between YneA and FtsW.

2.5 | ftsW-L148P bypasses yneA expression

Based on the observation that induced expression of *ftsW-L148P* suppressed YneA activity, we hypothesized that *ftsW-L148P* either prevents interaction with YneA or induces hyperactive cell division bypassing the YneA-induced checkpoint due to a change in conformation of the late divisome. Because FtsW is an essential protein with 10 transmembrane domains, we chose to measure cell length as a proxy to initiate division hyperactively in vivo. If FtsW-L148P is a variant that causes hyperactive cell division than cells expressing this variant should be shorter in the presence of DNA damage-induced YneA. Such a result would suggest that FtsW-L148P overcomes the YneA-induced checkpoint through a change in interaction with YneA, a change in peptidoglycan synthesis activity or a change in the divisome that initiates cell division hyperactively.

To test these ideas, we grew cells expressing *ftsW-L148P* or *ftsW* in a WT or Δ*ddcP*, Δ*ctpA*, Δ*ddcA* triple mutant background during normal growth or in the presence of DNA damage and measured cell length. Under conditions of normal growth, we did not observe a difference in cell length compared to WT when we induced *ftsW* and *ftsW-L148P* (Figures 5a and S3, Table S2). When we caused DNA damage with MMC, and therefore expression of native SOS-controlled *yneA*, we found that cells expressing both *ftsW-L148P* and *yneA* were shorter in length. We found that cells expressing *ftsW-L148P* (7.27 ± 1.64) are nearly 30% shorter than cells expressing *ftsW* (10.15 ± 2.97) and this difference was significant ($p = 4.71E^{-300}$; Figure 5b and Table S3). Given that *ftsW* does not bypass YneA activity, we would not expect the cell length of *ftsW* expressing cells in the triple mutant background to be much different than the triple mutant background alone. Indeed, we did not observe a reduction in the cell length of *ftsW* expressing cells in the triple mutant background (15.86 ± 4.89) compared to the triple mutant alone (16.5 ± 5.21; Figures 5b, S4 and Table S3). However, cell length is dramatically reduced in cells expressing *ftsW-L148P* in the triple mutant background (8.81 ± 2.43), a near 50% reduction in cell length, which is significantly different ($p = 2.6E^{-36}$; Figures 5b and S4, Table S3). With these results, we suggest the FtsW is unlikely to be a direct target of YneA. Instead, we suggest that *ftsW-L148P* generates a form of FtsW, which causes cell division to initiate hyperactively bypassing the inhibitory effect of YneA and preventing activation of the DNA damage checkpoint. Our result showing that *ftsW-L148P* does not result in shorter cells in the absence of DNA damage suggests the hyperactive cell division by FtsW-L148P either requires DNA damage to observe the effect or is more pronounced during conditions of damage when cell filamentation is extreme (Figure 5a and Table S2).

2.6 | YneA interacts with FtsL, Pbp2b, and Pbp1, but not FtsW

Given that cells expressing *ftsW-L148P* suppress YneA activity, we hypothesized that YneA either directly interacts with FtsW to inhibit cell division as observed for the *Caulobacter* proteins or FtsW-L148P encodes a hyperactive form of the protein as suggested above (Modell et al., 2011). We chose to assess interaction using the bacterial two-hybrid system (Karimova et al., 1998, 2017) as done previously to measure interaction between *Caulobacter* SidA and FtsW (Modell et al., 2011). As a positive control, it was previously shown that YneA and a catalytically inactive CtpA-S297A protease variant interact by bacterial two-hybrid analysis (Burby et al., 2018). We did not observe an interaction between YneA and FtsW or YneA and FtsW-L148P (Figure 6a,b). Since we did not detect a direct interaction between YneA and FtsW, we asked if YneA targets FtsW indirectly by interacting with other proteins involved in the late arriving divisome affecting cell division or peptidoglycan synthesis (Halbedel & Lewis, 2019; Kawai & Ogasawara, 2006; Król et al., 2012; Morales Angeles et al., 2020). First, we failed to observe an interaction between YneA and nine other proteins known to be involved in these processes (Figure 6a). We did, however, find a weak signal between YneA and FtsL suggesting an interaction may occur. When we switched the T25 and T18 fusions, we identified an interaction between YneA and FtsL, Pbp2b, and Pbp1 (Figure 6c). FtsL is an unstable late divisome component (Daniel & Errington, 2000). Pbp2b is a transpeptidase and Pbp1 is a bifunctional transpeptidase/transglycosylase (Popham & Setlow, 1995; Yanouri et al., 1993). FtsL, Pbp2b, and

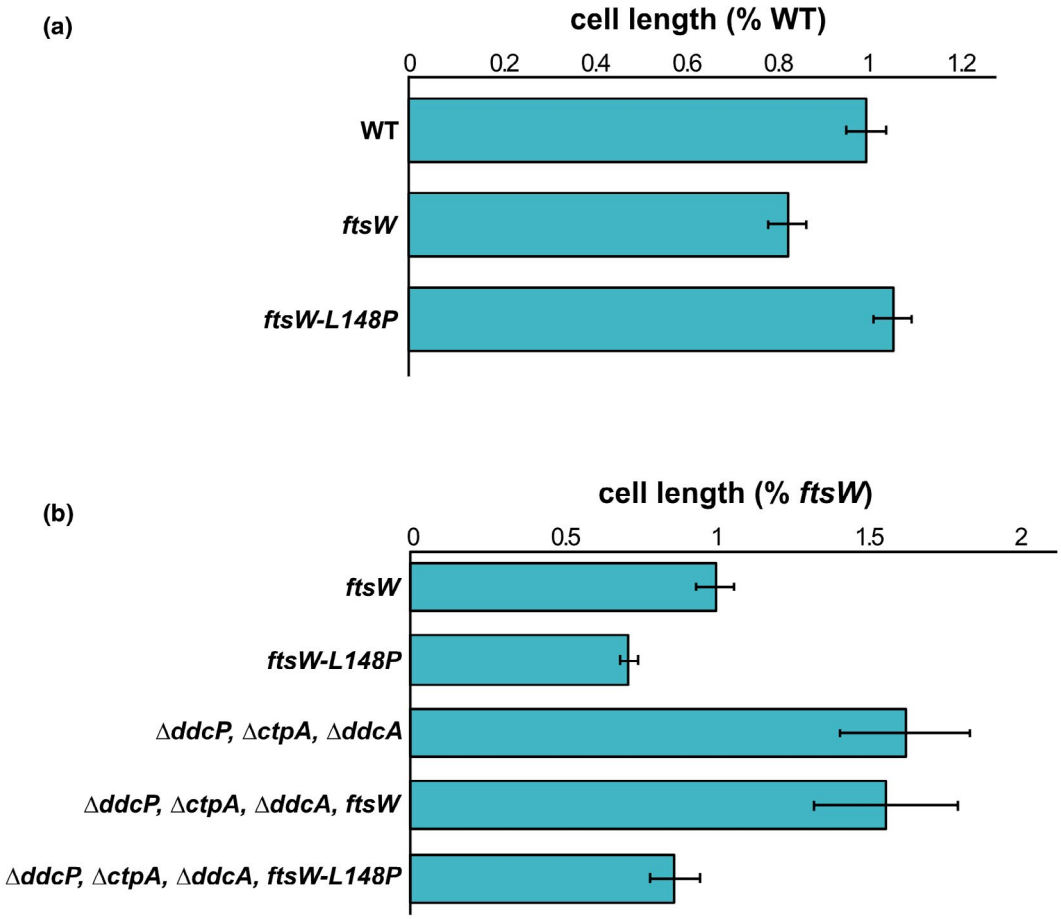

FIGURE 5 *ftsW-L148P* bypasses *yneA* expression. (a) Cell lengths of each strain relative to WT plotted as a bar graph during normal growth. Error bars represent standard error of the mean (*SEM*). The significance test are as follows for a two-tailed *t* test: PY79 and *amyE*::P_{hy}-*ftsW* ($p = .988$); PY79 and *amyE*::P_{hy}-*ftsW-L148P* ($p = .959$). (b) Cell lengths of each strain relative to *ftsW* plotted as a bar graph following addition of DNA damage (MMC). Error bars represent *SEM*. The significance tests are as follows for a two-tailed *t* test. For *amyE*::*Phy-ftsW* and *amyE*::*Phy-ftsW-L148P* ($p = 4.71E^{-300}$); *amyE*::*Phy-ftsW* and Δ*ddcP*, Δ*ctpA*, Δ*ddcA* ($p = 5.14E^{-119}$); *amyE*::*Phy-ftsW* and Δ*ddcP*, Δ*ctpA*, Δ*ddcA*, *amyE*::*Phy-ftsW-L148P* ($p = 2.6E^{-36}$). The cell length measurements graphed here are also presented in supporting Tables S2 and S3

Pbp1 all localize to the septum late during division contributing to the divisome or septal peptidoglycan synthesis (Bhambhani et al., 2020; Scheffers & Errington, 2004). These results suggest that YneA could indirectly effect FtsW through a direct interaction with one of these proteins contributing to DNA damage checkpoint enforcement.

2.7 | Mutations that prevent checkpoint activation and bypass yneA expression are less sensitive to an inhibitor of cell wall synthesis

Given that our results shown above suggest that YneA inhibits cell division by binding peptidoglycan through its LysM domain and through interaction with FtsL, Pbp2b, and Pbp1, we asked if cells expressing YneA are more sensitive to a cell wall antibiotic (Figure 7). If YneA prevents cell division by binding peptidoglycan then we would expect cells to be more sensitive to a cell wall inhibitor when YneA is expressed. Therefore, we treated cells with the inhibitor cephalexin, which restricts septal cell wall synthesis by preventing FtsI from crosslinking the glycan strands, but it does not directly damage the DNA (Modell et al., 2014). As a result, cephalexin will impede cell division, but independent of YneA. First, we treated cells with a low concentration of cephalexin in conjunction with increasing concentrations of IPTG and performed spot titer assays to assess if *yneA* expression affected growth in the presence of cephalexin (Figure 7a). We found that WT cells are unaffected by a low concentration of cephalexin; however, induction of *yneA* with increased concentrations of IPTG caused strong growth interference (Figure 7a,b). When we activate native *yneA* following treatment with MMC, cells are more sensitive to cephalexin (compare Figures 7b with 4d), and this proliferation defect is suppressed by Δ*yneA* (Figure 7b). To assess how the novel *yneA* alleles respond to cephalexin, we ectopically induced expression of each allele with increasing concentrations of IPTG in the absence of native *yneA*. At lower concentrations of IPTG, we found that each *yneA* mutant phenocopied the *yneA* null strain and suppressed the growth interference on cephalexin treatment (Figure 7b).

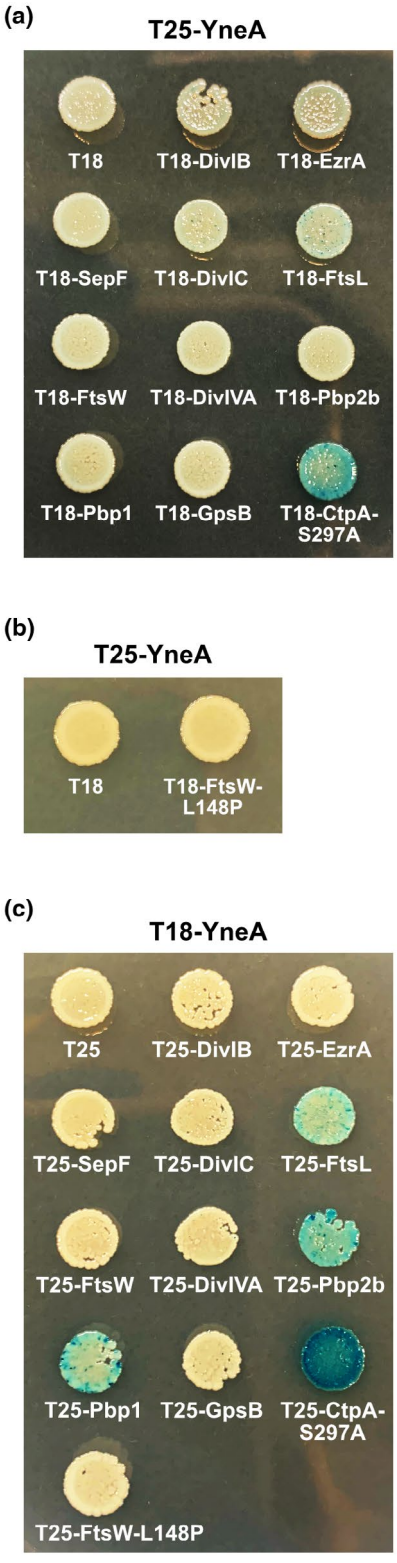

FIGURE 6 YneA interacts with FtsL, Pbp2b, and Pbp1. Bacterial two-hybrid assay using (a) empty vector (T18), T18 fusions and T25-YneA fusion; (b) empty vector (T18), T18-FtsW-L148P fusion, and T25-YneA fusion; (c) empty vector (T25), T25 fusions, and T18-YneA used to co-transform *E. coli*

To assess how *ftsW-L148P* responds to cephalexin, we ectopically induced WT *ftsW* and *ftsW-L148P* with IPTG in the presence of cephalexin. Similar to previous results, a low concentration of cephalexin does not hinder cell proliferation (Figure 7c). With the addition of MMC, WT cells are sensitive to cephalexin and are unable to continue proliferating (compare Figures 7d with 4d). However, induced expression of *ftsW-L148P* suppresses the effect of cephalexin and nearly phenocopied the *yneA* null strain (Figure 7d). These results support the conclusion that *ftsW-L148P* generates a hyperactive form of FtsW that is able to bypass the inhibitory effect of YneA and prevent activation of the DNA damage checkpoint. Further, our results showing that expression of YneA causes hypersensitivity to cephalexin support the model that part of the inhibitory effect of YneA on cell division is exerted through peptidoglycan binding by the YneA LysM domain.

3 | DISCUSSION

DNA damage checkpoints are ubiquitous across biology. In all organisms, the overarching process is to slow or arrest the cell cycle when DNA damage is detected enabling enough time for repair before chromosomes are segregated and cell division is complete. In bacteria, an SOS-induced protein enforces the DNA damage checkpoint by preventing cell division (for review, Burby & Simmons, 2020). In *E. coli*, SOS induced SulA blocks cell division by preventing FtsZ polymerization (Mukherjee et al., 1998); however, in *C. crescentus*, SidA and DidA do not affect FtsZ assembly, but instead delay cell division through a direct interaction with FtsW and FtsN, respectively (Modell et al., 2011, 2014). In *S. aureus*, SOS-induced SosA does not block the initial steps of septum formation but prevents the final steps of cell division (Bojer et al., 2019). In addition, previous two-hybrid analysis indicated possible interactions between SosA and factors required for cell division suggesting that like SidA and DidA protein–protein interactions are required for SosA-dependent checkpoint enforcement (Bojer et al., 2019; Modell et al., 2011). Therefore, the most prominent mechanism of checkpoint enforcement in bacteria invokes an interaction between an SOS-induced cell division inhibitor and a component of the divisome FtsZ, FtsW, or FtsN. In Caulobacter, some of the mutant forms for FtsW, I, and N that overcome SidA and DidA result in a mild decrease in cell length (4%–14%) suggesting that cell division can initiate hyperactively to some degree in these mutants as well (Modell et al., 2011). Based on our results, we suggest that YneA blocks cell division by targeting peptidoglycan through its LysM domain and by contact with FtsL, Pbp2b, and Pbp1 interfering with the ability of these proteins to properly function in cell division (Figure 8).

Another important feature of this work is our finding that loss of amino acid residues from the C-terminal tail up to the LysM domain decrease or prevent cells from responding to checkpoint enforcement (Figure 1). Previous work identified a point mutation in the extreme C-terminus that increased YneA stability and activity; however, removal of the entire C-terminal region of the protein, including the LysM domain, abolished YneA function (Mo & Burkholder, 2010). In line with the findings that full-length YneA is important to block cell division (Mo & Burkholder, 2010), we show that the Δ5 and Δ10 C-terminal truncations are stable suggesting that loss of portions of the C-terminal tail impairs YneA function. Because the C-terminal tail directly follows the LysM domain, we speculate that

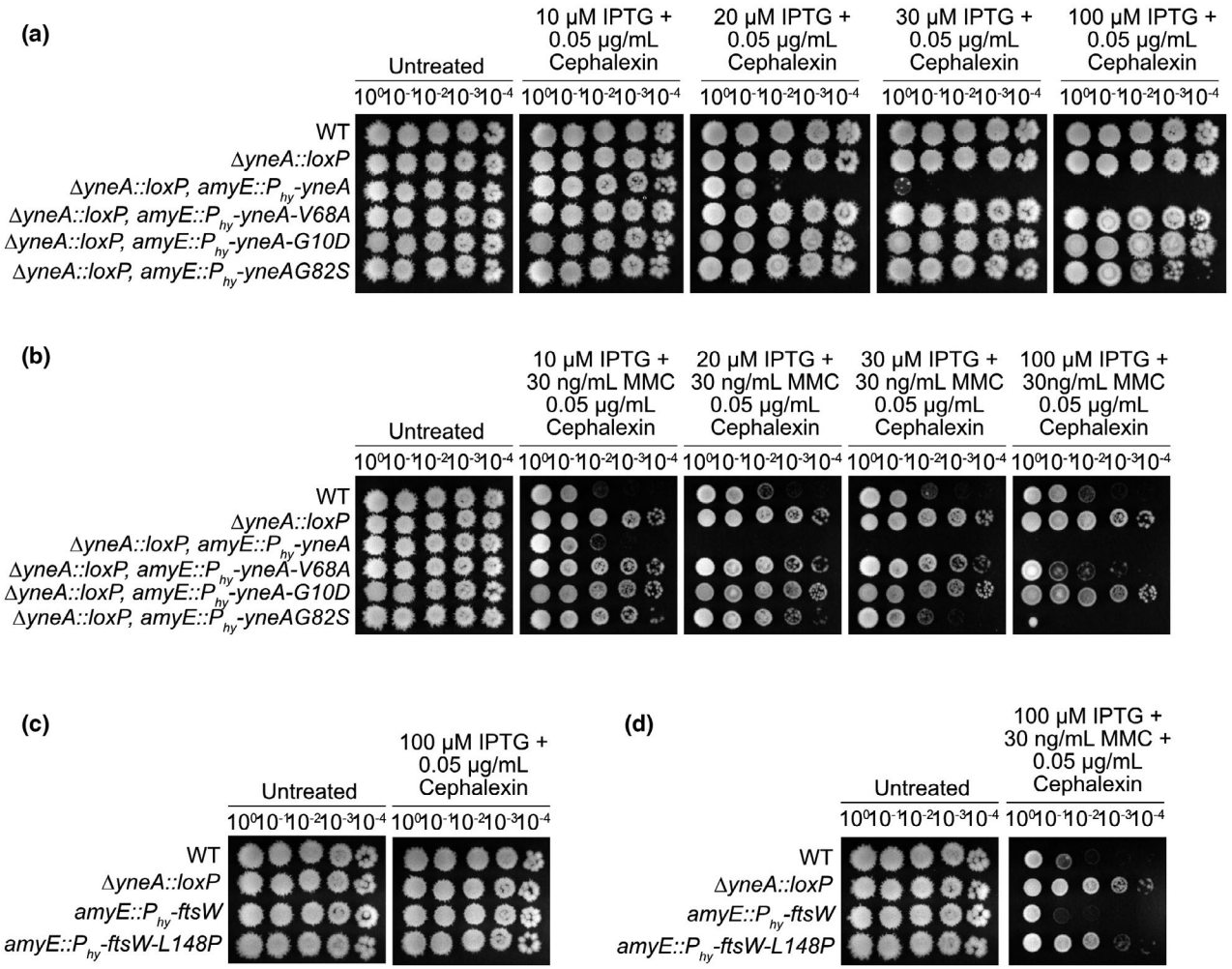

FIGURE 7 Mutations that prevent checkpoint activation and bypass *yneA* expression are less sensitive to an inhibitor of cell wall synthesis. Spot titer assay using *B. subtilis strains* (a and b) WT (PY79), Δ*yneA::loxP* (PEB439), Δ*yneA::loxP amyE::P*$_{hy}$*-yneA* (EAM46), Δ*yneA::loxP amyE::P*$_{hy}$*-yneA-V68A* (EAM49), Δ*yneA::loxP amyE::P*$_{hy}$*-yneA-G10D* (EAM50), and Δ*yneA::loxP amyE::P*$_{hy}$*-yneA-G82S* (EAM52); (c and d) WT (PY79), Δ*yneA::loxP* (PEB439), *amyE::P*$_{hy}$*-ftsW* (EAM72), and *amyE::P*$_{hy}$*-ftsW-L148P* (EAM69) spotted on the indicated media

the truncations may impair or alter LysM domain function. Another important finding is that *B. subtilis* cells show rather quick recovery from the DNA damage checkpoint (Burby et al., 2018). Our results demonstrating that loss of the C-terminal 15 amino acids ablates YneA function even though the protein can still be detected in cell extracts suggests that the quick recovery is in part mediated by protease-dependent truncation of the C-terminal tail. Therefore, we suggest that DdcP- and CtpA-mediated truncation of the C-terminal tail inactivates YneA quickly allowing cells to re-enter the cell cycle without requiring complete clearance of YneA from the septum.

We present a genetic selection for *yneA* mutants that fail to enforce the checkpoint identifying missense mutations with the only stable variants occurring in the LysM domain (Figure 2). Previous work identified several point mutations in the transmembrane domain that caused a reduction in YneA activity; furthermore, complete loss of the C-terminus, including the LysM domain, ablated YneA function (Mo & Burkholder, 2010). The LysM domain binds peptidoglycan and proteins that have LysM domains are often involved in remodeling the peptidoglycan cell wall (Buist et al., 2008). The analogous cell division inhibitor in *Mycobacterium tuberculosis*, Rv2719c (ChiZ), contains a LysM domain that was previously suggested to have peptidoglycan hydrolytic activity, although a recent report shows it does not (Chauhan et al., 2006; Escobar & Cross, 2018). The precise role of the LysM domain in YneA remains undetermined; however, our results show that single amino acid substitutions in the YneA LysM or a LysM domain swap abolish checkpoint enforcement even though the protein accumulates higher than WT levels in vivo. Our results considered with those of Mo and Burkholder demonstrate that integrity of the LysM domain is required for enforcement of the DNA damage checkpoint. We wish to note that most DNA damage-induced cell division inhibitors lack a LysM domain (Bojer et al., 2020; Burby & Simmons, 2020). SosA, DidA, and SidA lack LysM domains, and these proteins have been shown to interact with the cell wall synthesis machinery through a two-hybrid analysis indicating the mechanism of checkpoint enforcement is through protein–protein interactions (Bojer et al., 2019; Modell et al., 2011, 2014). Further, we show that expression of *yneA* strongly sensitizes cells to the cell wall antibiotic cephalexin. This result combined with our data showing that YneA

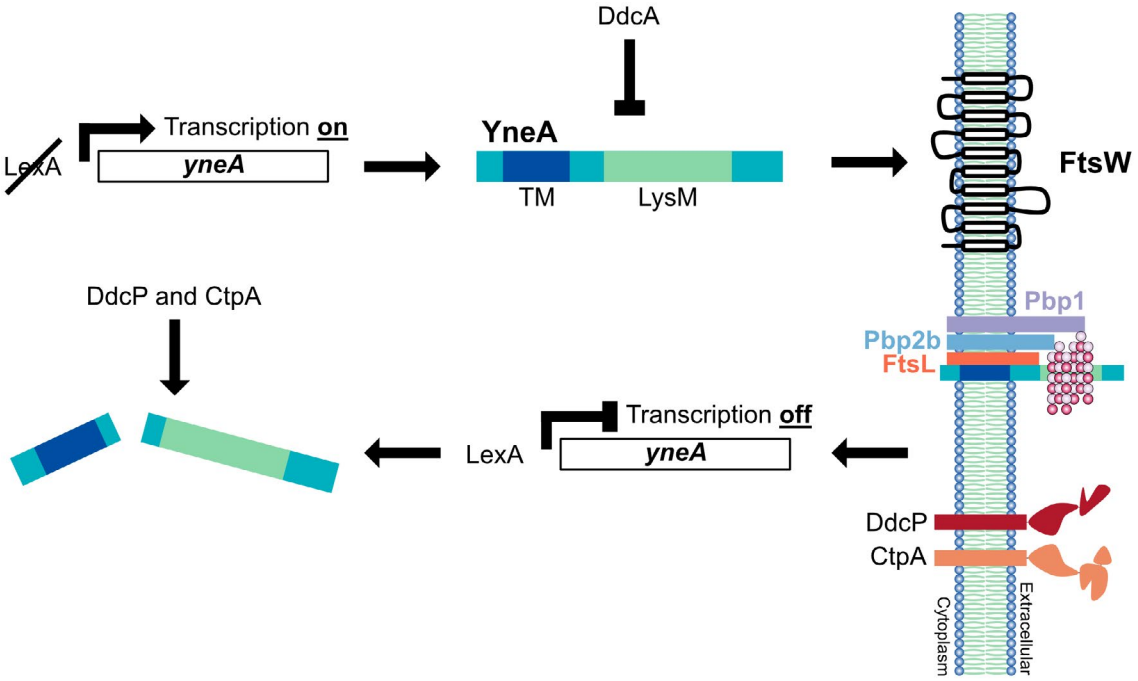

FIGURE 8 Model for YneA-induced cell division inhibition. In the presence of DNA damage, cleavage of LexA allows for expression of the SOS-induced cell division inhibitor YneA. YneA expression must reach a critical threshold to bypass the negative regulators DdcA, DdcP, and CtpA to activate the checkpoint. YneA localizes to the membrane, mediated by the transmembrane domain (TM), where it interacts with the late divisome proteins FtsL, Pbp2b, and Pbp1 as well as binds peptidoglycan interfering with cell wall remodeling at the septum. After the DNA is repaired and YneA expression is repressed by LexA, YneA is cleared by the proteases DdcP and CtpA allowing septal cell wall synthesis to commence and cell division to resume

LysM domain point mutants confer less sensitivity to cephalexin and *ftsW-L148P* phenocopies the *yneA* null strain on cephalexin suggests that an important part of checkpoint enforcement is interference of YneA with septal peptidoglycan synthesis.

In *M. tuberculosis*, it was previously shown that overexpression of ChiZ did not alter the amount of FtsZ or its activity; however, ChiZ did affect the organization of FtsZ at the septum. As a result, the authors speculated that the loss of peptidoglycan, mediated by ChiZ, at the site of cell wall synthesis could disrupt FtsZ localization and subsequent Z-ring formation (Chauhan et al., 2006). Interestingly, like ChiZ, overexpression of YneA did not change the level of FtsZ; however, YneA expression was reported to delay the assembly of FtsZ rings and/or the number of Z rings formed (Kawai et al., 2003; Mo & Burkholder, 2010). Bacterial two-hybrid analysis showed that ChiZ directly interacted with the cell division proteins FtsI and FtsQ, but not FtsZ (Vadrevu et al., 2011). Furthermore, a previous study was unable to detect a direct interaction between YneA and FtsZ by a two-hybrid assay; however, we detected an interaction between YneA and FtsL, Pbp2b and Pbp1 (Figure 6b; Kawai et al., 2003). We suggest that an important part of the YneA checkpoint enforcement mechanism is interfering with the ability of late divisome components FtsL, Pbp2B, and Pbp1 to interact. Our results suggest that part of the YneA inhibitory mechanism overlaps with that of Gp56 protein from bacteriophage SPO1 (Bhambhani et al., 2020).

We developed a genetic method using a selection followed by a secondary screen that yielded mutations in the *ftsW* gene, with most mutations impacting just two amino acid residues. Our characterization of *ftsW-L148P* shows that this variant completely bypassed the YneA-enforced DNA damage checkpoint including the cephalexin sensitivity (Figures 4 and 7). FtsW is an essential protein that is required for the polymerization of Lipid II into peptidoglycan during septal cell wall synthesis (Pastoret et al., 2004; Taguchi et al., 2019). Our results combined with the interactions we identified between YneA and other late divisome proteins suggest that *ftsW-L148P* encodes a hyperactive form of FtsW that is able to initiate division prematurely by stabilizing the late divisome components. In support of this model, in *E. coli*, it has been shown that mutations in FtsL and FtsA are also able to initiate cell division hyperactively (Geissler et al., 2007; Tsang & Bernhardt, 2015). In the case of the *ftsL* mutant the shorter cell length is a result of stabilization of late division components involved in septal peptidoglycan synthesis (Tsang & Bernhardt, 2015). For FtsA*, hyperactive initiation is through an increase in interaction between FtsA* and FtsZ (Geissler et al., 2007). In our work, induced expression of *ftsW-L148P* caused a substantial reduction in cell length compared to WT during the DNA damage response (Figure 5b). Given that we did not detect an interaction between YneA and FtsW or FtsW-L148P, but we did detect an interaction between YneA and other components of the divisome contributing to division and septal cell peptidoglycan synthesis (Figure 6a–c), we propose a model where YneA blocks cell division through both a direct protein–protein interaction with FtsL, Pbp2b, and Pbp1 and through binding to peptidoglycan using its LysM domain (Bhambhani et al., 2020). We further

suggest that *ftsW-L148P* overcomes YneA by stabilizing assembly of the late divisome complex. Our results provide new insight into how bacterial DNA damage checkpoints function. Since YneA is present in other organisms including the clinically relevant *Listeria monocytogenes*, these results may be applicable to understanding how certain bacteria are able to regulate cell proliferation under stress conditions.

4 | EXPERIMENTAL PROCEDURES

4.1 | Bacteriological methods and chemicals

Bacterial plasmids, oligonucleotides, and strains used in this study are listed in Tables S2–S4. Construction of individual strains is detailed in the supporting methods using double cross-over recombination as previously described (Burby & Simmons, 2017; Burby et al., 2018). All *B. subtilis* strains are isogenic derivatives of PY79 (Youngman et al., 1984). *B. subtilis* strains were grown in LB (10 g/L of NaCl, 10 g/L of tryptone, and 5 g/L of yeast extract) at 30°C with shaking (200 rpm). Individual plasmids were constructed using Gibson assembly as described previously (Gibson, 2011). The details of plasmid construction are described in the supporting information. Oligonucleotides used in this study were obtained from integrated DNA technologies. MMC (Fisher bioreagents) was used at the concentrations indicated in the figures. Cephalexin (Millipore Sigma) was used at the concentration indicated in the figures. Spectinomycin (100 μg/ml) was used for selection in *B. subtilis* as indicated in the method details. Selection of *E. coli* (MC1061 cells) transformants was performed using ampicillin (100 μg/ml).

4.2 | Transformation of PY79

PY79 was struck out on LB agar and incubated at 37°C overnight. A single colony was used to inoculate a 2 ml LM culture (LB + 3-mM $MgSO_4$) in a 14 ml round bottom culture tube. The culture was incubated at 37°C on a rolling rack until OD_{600} of approximately 1. Then, 150 μl of the LM culture was transferred to 3 ml pre-warmed MD media (1× PC buffer [107 g/L of K_2HPO_4, 60 g/L of KH_2PO_4, 11.8 g/L of trisodium citrate dihydrate], 2% glucose, 50 μg/ml of phenylalanine, 50 μg/ml of tryptophan, 11 μg/ml of ferric ammonium citrate, 2.5 mg/ml of sodium aspartate, 3 mM $MgSO_4$) and incubated on a rolling rack at 37°C for 4 hr. To each 3 ml competent cell culture, 2 μl of the designated plasmid or genomic DNA was added and the cultures were incubated on a rolling rack at 37°C for an additional 30 min. Transformations were plated on LB agar + 100 μg/ml of spectinomycin (200 μl/100-cm plate) and incubated at 30°C overnight.

4.3 | Strain construction

4.3.1 | General strain construction methods

All *B. subtilis* strains are isogenic derivatives of PY79 (Youngman et al., 1984) and were generated by transforming cells with a PCR product, plasmid DNA, or genomic DNA via natural competence (Harwood & Cutting, 1990).

Integration of inducible constructs at the *amyE* locus was achieved via double cross-over recombination. For constructs containing an IPTG-inducible promoter (P_{hy}), strains were transformed with plasmids or with genomic DNA of a strain already generated (see detailed strain construction) and transformants were selected using LB agar + 100 μg/ml of spectinomycin. Isolates were colony purified by re-streaking on LB agar + 100 μg/ml of spectinomycin. Incorporation via double cross-over at *amyE* was determined by PCR colony screen.

4.3.2 | Individual strain construction

See Supporting information.

4.4 | Plasmid construction

4.4.1 | General cloning techniques

Plasmids were assembled using Gibson assembly (Gibson, 2011). Gibson assembly reactions were 20 μl consisting of 1× Gibson assembly master mix (0.1 M Tris pH 8.0, 5% PEG-8000, 10 mM $MgCl_2$, 10 mM DTT, 0.2 mM dNTPs, 1 mM NAD^+, 4 units/ml of T_5 exonuclease, 25 units/ml of Phusion DNA polymerase, 4,000 units/ml of Taq DNA ligase) and 40–100 ng of each PCR product and incubated at 50°C for 60 min. All PCR products were isolated via gel extraction from an agarose gel. Gibson assembly reactions were used to transform MC1061 *E. coli*.

4.4.2 | Individual plasmid construction

See Supporting information.

4.5 | Spot titer assays

B. subtilis strains were struck out on LB agar and incubated at 30°C overnight. The next day, a single colony was used to inoculate a 2 ml LB culture in a 14 ml round bottom culture tube, which was incubated at 37°C on a rolling rack until OD_{600} was 0.5–1. Cultures were normalized to OD_{600} = 0.5 and serial diluted. The serial dilutions were spotted (5 μl) on the LB agar plates indicated in the figures, and the plates were incubated at 30°C overnight (16–20 hr). All spot titer assays were performed at least three times.

4.6 | Western blotting

For overexpression of YneA, cultures of LB were inoculated at an OD_{600} = 0.2 and 1 mM IPTG final concentration was added. Cultures

were incubated at 30°C. Samples of an $OD_{600} = 1$ were harvested and washed one time with 1× PBS pH 7.4. Samples were re-suspended in 100 µl 1× SMM buffer (0.5 M sucrose, 0.02 M maleic acid, 0.02 M $MgCl_2$, adjusted o PH 6.5) containing 100 units/ml of mutanolysin and 2× Roche protease inhibitors. Samples were incubated at 37°C for 2 hr. SDS sample buffer was added to 1× and incubated at 100°C for 7 min. Samples (12 µl) were separated via 10% SDS-PAGE and transferred to nitrocellulose using a Trans-Blot Turbo (BioRad) according to the manufacturer's directions. Membranes were blocked in 5% milk in tris-buffered saline and Tween (TBST) (25 mM Tris, pH 7.5, 150 mM NaCl and 0.1% Tween 20) at room temperature for 1 hr. Blocking buffer was removed and primary antibodies were added in 2% milk in TBST (αYneA, 1:3,000; αDnaN, 1:4,000). Primary antibody incubation was performed at room temperature for 1 hr. Primary antibodies were removed, and membranes were washed three times with TBST for 5 min at room temperature. Secondary antibodies (Licor, 1:15,000) were added in 2% milk in TBST and incubated at room temperature for 1 hr. Membranes were washed three times as above and imaged using Li-COR Odyssey imaging system. All western blot experiments were performed at least three times with independent samples. Molecular weight markers were used in the YneA and DnaN blots.

4.7 | Microscopy

Strains were grown on LB agar plates at 30° overnight. Plates were washed with LB media and cultures of LB were inoculated at an OD_{600} = 0.1 and incubated at 30° until OD_{600} of about 0.2 when MMC was added at 100 ng/ml of final concentration, and cultures were induced with 1-mM IPTG final concentration and incubated at 30° until OD_{600} of 0.6–0.8. Samples were taken and incubated with 4 µg/ml of FM4-64 for 5 min and transferred to pads of 1× Spizizen salts and 1% agarose. Images were captured with an Olympus BX61 microscope (Burby et al., 2018, 2019).

4.8 | FtsW suppressor identification

The parent strain for the *yneA* overexpression suppressor screen was PEB852, a derivative of PY79 with *ddcP*, *ctpA*, and *ddcA* genes deleted and ectopic expression of *yneA* under the control of a xylose inducible promoter inserted into the *amyE* locus. PEB852 was grown on an LB plate with 5 µg/ml of chloramphenicol overnight. The next day, the plate was washed with LB and used to inoculate a 10 ml LB culture to an OD_{600} of 0.05. The culture was grown to OD ~1 and used to inoculate multiple 10 ml LB cultures to OD 0.05. These source flasks were grown to an OD_{600} of 2 at 30°C. At this point, cells were pelleted and stored for DNA extraction, and glycerol stocks were prepared. Later 100 µl of 10^{-1} diluted cells were used to inoculate three 0.2% xylose LB plates per source flask. Colonies capable of growing on the initial xylose LB plates were restruck onto new 0.2% xylose LB plates and allowed to grow overnight. Those that grew on the secondary xylose plates were then struck on plates with 20 ng/ml of MMC. Colonies that grew on MMC were saved as glycerol stocks and eventually sequenced. This screen was preformed twice. The first utilized five source flasks which were named WDH1-5 and yielded three mutants capable of growth in both conditions; these isolates were named WDH6-8. The second iteration of the screen was scaled up to 10 source flasks named WDH9-18 and yielded 27 mutants which were named WDH19-45.

All xylose/MMC growing mutants and the mutant-yielding source flasks were sent for NovaSeq H4K paired end 75 cycle sequencing at the University of Michigan core. The sequencing results were analyzed by breseq (Deatherage & Barrick, 2014) on the Flux computing cluster. This analysis revealed that all but one of the mutants had a mutation in *ftsW*. The one mutant that did not had no detectable mutations beyond baseline. Other mutations were detected in some isolates (Table S1) but never without an accompanying *ftsW* mutation, and no other gene or intergenic locus was found to be mutated in more than one isolate. Of the 29 detected *ftsW* mutations, 20 occurred at amino acid 158 and seven occurred at or near amino acid 148 indicating two potentially important residues. All raw sequencing files are publicly available BioProject # PRJNA707525 (http://www.ncbi.nlm.nih.gov/bioproject) ([Dataset], Hawkins et al., 2021).

4.9 | Bacterial two-hybrid

Plasmids used for bacterial two-hybrid assay are listed in Table S4. Bacterial two-hybrid assays were performed as previously described (Burby et al., 2018; Matthews & Simmons, 2019). T18 and T25 fusion plasmids (details of the specific plasmids used can be viewed in Table S4) were used to co-transform BTH101 cells, and co-transformants were selected on LB agar + 100 µg/ml of ampicillin + 25 µg/ml of kanamycin at 37°C overnight. Co-transformants were grown in 3 ml of LB media (supplemented with 100 µg/ml of ampicillin and 25 µg/ml of kanamycin) at 37°C until an OD_{600} of between 0.5 and 1.0 was reached. The cultures were adjusted to an OD_{600} of 0.5, diluted 1/1000 in LB and spotted (5 µl/spot) onto LB agar plates containing 40 µg/ml of X-Gal (5-bromo-4-chloro-3-indox y-β-D-galactopyranoside), 0.5 mM IPTG, 100 µg/ml of ampicillin, and 25 µg/ml of kanamycin. The plates were incubated for two days at 30°C followed by an additional 24 hr at room temperature while being protected from light. All two-hybrid experiments were performed a minimum of three times working from fresh co-transformations.

ACKNOWLEDGMENTS

We would like to thank members of the Simmons lab for their helpful discussions. PEB was supported by a predoctoral fellowship #DGE1256260 from the National Science Foundation. PEB and JSL were also supported by Rackham Predoctoral Fellowships and BRG was supported in part by an MCDB Summer Undergraduate Research Fellowship. The National Institutes of Health grant R35 GM131772 to LAS supported this work.

CONFLICT OF INTEREST

The authors have no conflict of interest to declare.

AUTHOR CONTRIBUTIONS

This study was conceived and designed by E.A. Masser, P.E. Burby, W.D. Hawkins, B.R. Gustafson, J.S. Lenhart, and L.A. Simmons. Experiments were performed by E.A. Masser, P.E. Burby, W.D. Hawkins, B.R. Gustafson, and J.S. Lenhart. Data analysis was performed by E.A. Masser, P.E. Burby, W.D. Hawkins, B.R. Gustafson, J.S. Lenhart, and L.A. Simmons. The experiments shown in Figures 1–7 and S1–S4 were performed by E.A. Masser except 4B. The genetic method for isolation of *ftsW* mutations was conceived by P.E. Burby and performed by P.E. Burby and W.D. Hawkins. The selection for *yneA* point mutations was originally performed by B.R. Gustafson and J.S. Lenhart. The first manuscript draft was written by E.A. Masser and L.A. Simmons. All other authors contributed to the final version.

DATA AVAILABILITY STATEMENT

All data relevant to this study is presented in the main text or supporting information. The whole genome sequence data used to identify the *ftsW* mutations have been deposited at SRA and are available through BioProject # PRJNA707525. The BioProject covers accession numbers SAMN18208222 through SAMN18208263 and can be found at the following site (http://www.ncbi.nlm.nih.gov/bioproject; [Dataset], Hawkins et al., 2021). Any strain, sequence or other material or information used in this study is available upon request.

ORCID

Lyle A. Simmons https://orcid.org/0000-0002-9600-7623

REFERENCES

Au, N., Kuester-Schoeck, E., Mandava, V., Bothwell, L.E., Canny, S.P., Chachu, K. et al. (2005) Genetic composition of the *Bacillus subtilis* SOS system. *Journal of Bacteriology*, *187*(22), 7655–7666.

Bhambhani, A., Iadicicco, I., Lee, J., Ahmed, S., Belfatto, M., Held, D. et al. (2020) Bacteriophage SP01 gene product 56 inhibits *Bacillus subtilis* cell division by interacting with FtsL and disrupting Pbp2B and FtsW recruitment. *Journal of Bacteriology*, *203*(2), e00463-20. https://doi.org/10.1128/JB.00463-20

Bojer, M.S., Frees, D. & Ingmer, H. (2020) SosA in Staphylococci: an addition to the paradigm of membrane-localized, SOS-induced cell division inhibition in bacteria. *Current Genetics*, *66*(3), 495–499. https://doi.org/10.1007/s00294-019-01052-z

Bojer, M.S., Wacnik, K., Kjelgaard, P., Gallay, C., Bottomley, A.L., Cohn, M.T. et al. (2019) SosA inhibits cell division in *Staphylococcus aureus* in response to DNA damage. *Molecular Microbiology*, *112*(4), 1116–1130.

Bridges, B.A. (1995) Are there DNA damage checkpoints in *E. coli*? *BioEssays*, *17*(1), 63–70. https://doi.org/10.1002/bies.950170112

Buist, G., Steen, A., Kok, J. & Kuipers, O.P. (2008) LysM, a widely distributed protein motif for binding to (peptido)glycans. *Molecular Microbiology*, *68*(4), 838–847. https://doi.org/10.1111/j.1365-2958.2008.06211.x

Burby, P.E. & Simmons, L.A. (2017) CRISPR/Cas9 editing of the *Bacillus subtilis* genome. *Bio Protocol*, *7*(8), e2272. https://doi.org/10.21769/BioProtoc.2272

Burby, P.E. & Simmons, L.A. (2020) Regulation of cell division in bacteria by monitoring genome integrity and DNA replication status. *Journal of Bacteriology*, *202*(2), e00408-19. https://doi.org/10.1128/JB.00408-19

Burby, P.E., Simmons, Z.W., Schroeder, J.W. & Simmons, L.A. (2018) Discovery of a dual protease mechanism that promotes DNA damage checkpoint recovery. *PLoS Genetics*, *14*(7), e1007512.

Burby, P.E., Simmons, Z.W. & Simmons, L.A. (2019) DdcA antagonizes a bacterial DNA damage checkpoint. *Molecular Microbiology*, *111*(1), 237–253. https://doi.org/10.1111/mmi.14151

Chauhan, A., Lofton, H., Maloney, E., Moore, J., Fol, M., Madiraju, M.V. et al. (2006) Interference of *Mycobacterium tuberculosis* cell division by Rv2719c, a cell wall hydrolase. *Molecular Microbiology*, *62*(1), 132–147. https://doi.org/10.1111/j.1365-2958.2006.05333.x

Ciccia, A. & Elledge, S.J. (2010) The DNA damage response: making it safe to play with knives. *Molecular Cell*, *40*(2), 179–204. https://doi.org/10.1016/j.molcel.2010.09.019

Cole, S.T. (1983) Characterization of the promoter for the LexA regulated *sulA* gene of *Escherichia coli*. *Molecular and General Genetics*, *189*, 400–404.

Daniel, R.A. & Errington, J. (2000) Intrinsic instability of the essential cell division protein FtsL of *Bacillus subtilis* and a role for DivIB protein in FtsL turnover. *Molecular Microbiology*, *36*(2), 278–289. https://doi.org/10.1046/j.1365-2958.2000.01857.x

Deatherage, D.E. & Barrick, J.E. (2014) Identification of mutations in laboratory-evolved microbes from next-generation sequencing data using breseq. *Methods in Molecular Biology*, *1151*, 165–188.

Escobar, C.A. & Cross, T.A. (2018) False positives in using the zymogram assay for identification of peptidoglycan hydrolases. *Analytical Biochemistry*, *543*, 162–166.

Friedberg, E.C., Walker, G.C., Siede, W., Wood, R.D., Schultz, R.A. & Ellenberger, T. (2006) *DNA repair and mutagenesis*, 2nd edition, : American Society for Microbiology.

Geissler, B., Shiomi, D. & Margolin, W. (2007) The ftsA* gain-of-function allele of *Escherichia coli* and its effects on the stability and dynamics of the Z ring. *Microbiology (Reading)*, *153*(Pt 3), 814–825.

Gibson, D.G. (2011) Enzymatic assembly of overlapping DNA fragments. *Methods in Enzymology*, *498*, 349–361.

Halbedel, S. & Lewis, R.J. (2019) Structural basis for interaction of DivIVA/GpsB proteins with their ligands. *Molecular Microbiology*, *111*(6), 1404–1415. https://doi.org/10.1111/mmi.14244

Harwood, C.R. & Cutting, S.M. (1990) *Molecular biological methods for Bacillus*. New York: Wiley.

Hawkins, W.D., Burby, P.E. & Simmons, L.A. (2021) *Whole-genome sequencing coverage for identification of ftsW mutations*. [Dataset] SRA BioProject.

Iyer, V.N. & Szybalski, W. (1963) A molecular mechanism of mitomycin action: linking of complementary DNA strands. *Proceedings of the National Academy of Sciences of the United States of America*, *50*, 355–362.

Karimova, G., Gauliard, E., Davi, M., Ouellette, S.P. & Ladant, D. (2017) Protein-protein interaction: bacterial two-hybrid. *Methods in Molecular Biology*, *1615*, 159–176.

Karimova, G., Pidoux, J., Ullmann, A. & Ladant, D. (1998) A bacterial two-hybrid system based on a reconstituted signal transduction pathway. *Proceedings of the National Academy of Sciences of the United States of America*, *95*(10), 5752–5756. https://doi.org/10.1073/pnas.95.10.5752

Kawai, Y., Moriya, S. & Ogasawara, N. (2003) Identification of a protein, YneA, responsible for cell division suppression during the SOS response in *Bacillus subtilis*. *Molecular Microbiology*, *47*(4), 1113–1122. https://doi.org/10.1046/j.1365-2958.2003.03360.x

Kawai, Y. & Ogasawara, N. (2006) *Bacillus subtilis* EzrA and FtsL synergistically regulate FtsZ ring dynamics during cell division. *Microbiology (Reading)*, *152*(Pt 4), 1129–1141.

Król, E., van Kessel, S.P., van Bezouwen, L.S., Kumar, N., Boekema, E.J. & Scheffers, D.J. (2012) *Bacillus subtilis* SepF binds to the C-terminus of FtsZ. *PLoS One*, *7*(8), e43293.

Lenhart, J.S., Schroeder, J.W., Walsh, B.W. & Simmons, L.A. (2012) DNA repair and genome maintenance in *Bacillus subtilis*. *Microbiology and Molecular Biology Reviews*, *76*(3), 530–564. https://doi.org/10.1128/MMBR.05020-11

Little, J.W. & Gellert, M. (1983) The SOS regulatory system: control of its state by the level of RecA protease. *Journal of Molecular Biology*, *167*(4), 791–808. https://doi.org/10.1016/S0022-2836(83)80111-9

Matthews, L.A. & Simmons, L.A. (2019) Cryptic protein interactions regulate DNA replication initiation. *Molecular Microbiology*, *111*(1), 118–130. https://doi.org/10.1111/mmi.14142

Mizusawa, S., Court, D. & Gottesman, S. (1983) Transcription of the *sulA* gene and repression by LexA. *Journal of Molecular Biology*, *171*, 337–343.

Mizusawa, S. & Gottesman, S. (1983) Protein degradation in *Escherichia coli*: the lon gene controls the stability of sulA protein. *Proceedings of the National Academy of Sciences of the United States of America*, *80*(2), 358–362. https://doi.org/10.1073/pnas.80.2.358

Mo, A.H. & Burkholder, W.F. (2010) YneA, an SOS-induced inhibitor of cell division in *Bacillus subtilis*, is regulated posttranslationally and requires the transmembrane region for activity. *Journal of Bacteriology*, *192*(12), 3159–3173.

Modell, J.W., Hopkins, A.C. & Laub, M.T. (2011) A DNA damage checkpoint in *Caulobacter crescentus* inhibits cell division through a direct interaction with FtsW. *Genes & Development*, *25*(12), 1328–1343. https://doi.org/10.1101/gad.2038911

Modell, J.W., Kambara, T.K., Perchuk, B.S. & Laub, M.T. (2014) A DNA damage-induced, SOS-independent checkpoint regulates cell division in *Caulobacter crescentus*. *PLoS Biology*, *12*(10), e1001977.

Morales Angeles, D., Macia-Valero, A., Bohorquez, L.C. & Scheffers, D.J. (2020) The PASTA domains of *Bacillus subtilis* PBP2B strengthen the interaction of PBP2B with DivIB. *Microbiology (Reading)*, *166*(9), 826–836.

Mukherjee, A., Cao, C. & Lutkenhaus, J. (1998) Inhibition of FtsZ polymerization by SulA, an inhibitor of septation in *Escherichia coli*. *Proceedings of the National Academy of Sciences of the United States of America*, *95*(6), 2885–2890. https://doi.org/10.1073/pnas.95.6.2885

Noll, D.M., Mason, T.M. & Miller, P.S. (2006) Formation and repair of interstrand cross-links in DNA. *Chemical Reviews*, *106*(2), 277–301. https://doi.org/10.1021/cr040478b

Pastoret, S., Fraipont, C., den Blaauwen, T., Wolf, B., Aarsman, M.E., Piette, A. et al. (2004) Functional analysis of the cell division protein FtsW of *Escherichia coli*. *Journal of Bacteriology*, *186*(24), 8370–8379.

Pereira, F.C., Nunes, F., Cruz, F., Fernandes, C., Isidro, A.L., Lousa, D. et al. (2019) A LysM domain intervenes in sequential protein-protein and protein-peptidoglycan interactions important for spore coat assembly in *Bacillus subtilis*. *Journal of Bacteriology*, *201*(4), e00642-18. https://doi.org/10.1128/JB.00642-18

Popham, D.L. & Setlow, P. (1995) Cloning, nucleotide sequence, and mutagenesis of the *Bacillus subtilis* ponA operon, which codes for penicillin-binding protein (PBP) 1 and a PBP-related factor. *Journal of Bacteriology*, *177*(2), 326–335. https://doi.org/10.1128/jb.177.2.326-335.1995

Scheffers, D.J. & Errington, J. (2004) PBP1 is a component of the *Bacillus subtilis* cell division machinery. *Journal of Bacteriology*, *186*(15), 5153–5156.

Simmons, L.A., Foti, J.J., Cohen, S.E. & Walker, G.C. (2008) The SOS regulatory network. *EcoSal Plus*, *3*(1), 1–30.

Simmons, L.A., Grossman, A.D. & Walker, G.C. (2007) Replication is required for the RecA localization response to DNA damage in *Bacillus subtilis*. *Proceedings of the National Academy of Sciences of the United States of America*, *104*(4), 1360–1365. https://doi.org/10.1073/pnas.0607123104

Sutton, M.D., Smith, B.T., Godoy, V.G. & Walker, G.C. (2000) The SOS response: recent insights into umuDC-dependent mutagenesis and DNA damage tolerance. *Annual Review of Genetics*, *34*, 479–497.

Taguchi, A., Welsh, M.A., Marmont, L.S., Lee, W., Sjodt, M., Kruse, A.C. et al. (2019) FtsW is a peptidoglycan polymerase that is functional only in complex with its cognate penicillin-binding protein. *Nature Microbiology*, *4*(4), 587–594. https://doi.org/10.1038/s41564-018-0345-x

Tsang, M.J. & Bernhardt, T.G. (2015) A role for the FtsQLB complex in cytokinetic ring activation revealed by an FtsL allele that accelerates division. *Molecular Microbiology*, *95*(6), 925–944.

Vadrevu, I.S., Lofton, H., Sarva, K., Blasczyk, E., Plocinska, R., Chinnaswamy, J. et al. (2011) ChiZ levels modulate cell division process in mycobacteria. *Tuberculosis (Edinburgh)*, *91*(Suppl 1), S128–S135.

Walker, G.C., Smith, B.T. & Sutton, M.D. (2000) The SOS response to DNA damage.In: Storz, G. & Hengge-Aronis, R. (Eds.) *Bacterial stress responses*. : The American Society for Microbiology, pp. 131–144.

Yanouri, A., Daniel, R.A., Errington, J. & Buchanan, C.E. (1993) Cloning and sequencing of the cell division gene pbpB, which encodes penicillin-binding protein 2B in *Bacillus subtilis*. *Journal of Bacteriology*, *175*(23), 7604–7616. https://doi.org/10.1128/jb.175.23.7604-7616.1993

Youngman, P., Perkins, J.B. & Losick, R. (1984) Construction of a cloning site near one end of Tn917 into which foreign DNA may be inserted without affecting transposition in *Bacillus subtilis* or expression of the transposon-borne erm gene. *Plasmid*, *12*(1), 1–9. https://doi.org/10.1016/0147-619X(84)90061-1

SUPPORTING INFORMATION

Additional Supporting Information may be found online in the Supporting Information section.

How to cite this article: Masser, E.A., Burby, P.E., Hawkins, W.D., Gustafson, B.R., Lenhart, J.S. & Simmons, L.A. (2021) DNA damage checkpoint activation affects peptidoglycan synthesis and late divisome components in *Bacillus subtilis*. *Molecular Microbiology*, 116, 707–722. https://doi.org/10.1111/mmi.14765